

# ADVANCED TOKAMAK RESEARCH IN DIII-D

by

C.M. GREENFIELD, M. MURAKAMI, J.R. FERRON, M.R. WADE, T.C. LUCE, C.C. PETTY,  
J.E. MENARD, T.W. PETRIE, S.L. ALLEN, K.H. BURRELL, T.A. CASPER, J.C. DeBOO,  
E.J. DOYLE, A.M. GAROFALO, I.A. GORELOV, R.J. GROEBNER, J. HOBIRK,  
A.W. HYATT, R.J. JAYAKUMAR, C.E. KESSEL,<sup>†</sup> R.J. LA HAYE, G.L. JACKSON,  
L.L. LAO, J. LOHR, M.A. MAKOWSKI, R.I. PINSKER, P.A. POLITZER, R. PRATER,  
G.M. STAEBLER, E.J. STRAIT, T.S. TAYLOR, W.P. WEST, and the DIII-D TEAM

JUNE 2004

## DISCLAIMER

This report was prepared as an account of work sponsored by an agency of the United States Government. Neither the United States Government nor any agency thereof, nor any of their employees, makes any warranty, express or implied, or assumes any legal liability or responsibility for the accuracy, completeness, or usefulness of any information, apparatus, product, or process disclosed, or represents that its use would not infringe privately owned rights. Reference herein to any specific commercial product, process, or service by trade name, trademark, manufacturer, or otherwise, does not necessarily constitute or imply its endorsement, recommendation, or favoring by the United States Government or any agency thereof. The views and opinions of authors expressed herein do not necessarily state or reflect those of the United States Government or any agency thereof.

# ADVANCED TOKAMAK RESEARCH IN DIII-D

by

C.M. GREENFIELD, M. MURAKAMI,\* J.R. FERRON, M.R. WADE,\* T.C. LUCE, C.C. PETTY,  
J.E. MENARD,† T.W. PETRIE, S.L. ALLEN,‡ K.H. BURRELL, T.A. CASPER,‡ J.C. DeBOO,  
E.J. DOYLE,Δ A.M. GAROFALO,# I.A. GORELOV, R.J. GROEBNER, J. HOBIRK,§  
A.W. HYATT, R.J. JAYAKUMAR,‡ C.E. KESSEL,† R.J. LA HAYE, G.L. JACKSON,  
L.L. LAO, J. LOHR, M.A. MAKOWSKI, R.I. PINSKER, P.A. POLITZER, R. PRATER,  
G.M. STAEBLER, E.J. STRAIT, T.S. TAYLOR, W.P. WEST, and the DIII-D TEAM

This is a preprint of a paper to be presented at the 31<sup>st</sup> European Conf. on Plasma Physics and Controlled Fusion, London, United Kingdom, June 28 through July 2, 2004 and to be published in the *Plasma Physics and Controlled Fusion*.

\*Oak Ridge National Laboratory, Oak Ridge, Tennessee.

†Princeton Plasma Physics Laboratory, Princeton, New Jersey.

‡Lawrence Livermore National Laboratory, Livermore, California.

ΔUniversity of California, Los Angeles, California.

#Columbia University, New York, New York.

§Max Planck Institute for Plasma Physics, Garching, Germany.

Work supported by  
the U.S. Department of Energy under  
DE-FC02-04ER54698, DE-AC05-00OR22725, DE-AC02-76CH03073,  
W-7405-ENG-48, DE-FG03-01ER54615, and DE-FG02-89ER53297

GENERAL ATOMICS PROJECT 30200  
JUNE 2004

## ABSTRACT

Advanced Tokamak (AT) research in DIII-D seeks to provide a scientific basis for steady-state high performance operation in future devices. These regimes require high toroidal beta to maximize fusion output and high poloidal beta to maximize the self-driven bootstrap current. Achieving these conditions requires integrated, simultaneous control of the current and pressure profiles, and active magnetohydrodynamic (MHD) stability control. The building blocks for AT operation are in hand. Resistive wall mode stabilization via plasma rotation and active feedback with non-axisymmetric coils allows routine operation above the no-wall beta limit. Neoclassical tearing modes are stabilized by active feedback control of localized electron cyclotron current drive (ECCD). Plasma shaping and profile control provide further improvements. Under these conditions, bootstrap supplies most of the current. Steady-state operation requires replacing the remaining inductively driven current, mostly located near the half radius, with noninductive external sources. In DIII-D this current is provided by ECCD, and nearly stationary AT discharges have been sustained with little remaining inductive current. Fast wave current drive is being developed to control the central magnetic shear. Density control, with divertor cryopumps, of AT discharges with ELMing H-mode edges facilitates high current drive efficiency at reactor relevant collisionalities. An advanced plasma control system allows integrated control of these elements. Close coupling between modeling and experiment is key to understanding the separate elements, their complex nonlinear interactions, and their integration into self-consistent high performance scenarios. This approach has resulted in fully noninductively driven plasmas with  $\beta_N \leq 3.5$  and  $\beta_T \leq 3.6\%$  sustained for up to 1 second, approximately one current relaxation time. Progress in this area, and its implications for next-step devices, will be illustrated by results of these and other recent experiment and simulation efforts.

## I. INTRODUCTION

A major goal of next-step fusion devices such as ITER will be the demonstration of sufficient fusion performance to point toward the use of fusion as an economical energy source. At present, conventional H-mode scenarios appear capable of fulfilling this requirement. However, the dependence of such scenarios on a transformer to drive most of their current makes these scenarios inherently pulsed. Advanced Tokamak (AT) efforts [1,2] in DIII-D and elsewhere [3,4] focus on developing regimes that can operate in steady state at levels of fusion performance comparable to the conventional H-mode.

It may be noted that another class of advanced scenarios, the “hybrid” mode of operation, is under study in DIII-D [5] and elsewhere [6]. These discharges are characterized by stationary operation with high performance, but still have considerable inductive current and so do not aim at steady-state.

For steady-state operation, all of the plasma current must be supplied by noninductive means. To minimize the dependence on external noninductive current drive systems, the self-generated bootstrap current [7],  $I_{BS}$ , must be relied upon to provide most of the plasma current. Otherwise, the cost and power consumption of external systems could become prohibitive. The fraction of bootstrap current,  $f_{BS} = I_{BS}/I_p \propto \beta_p \propto q\beta_N$ , must be large. Here  $\beta_p = 2\mu_0 \langle p \rangle / B_p^2$  is the ratio of the plasma pressure to the poloidal magnetic field pressure,  $\beta_N = aB_T\beta_T/I_p$  is the normalized beta (with minor radius  $a$  in m, toroidal magnetic field  $B_T$  in T,  $\beta_T$  in percent and plasma current  $I_p$  in MA) and  $\beta_T = 2\mu_0 \langle p \rangle / B_T^2$  is the toroidal beta. The need for a well-aligned bootstrap further constrains the plasma conditions: not only should  $\beta_p$  be large, but the kinetic profiles must also be broad to produce a bootstrap current profile consistent with the desired current profile shape. The remainder of the plasma current is provided by external, noninductive means.

In the Advanced Tokamak we operate at the highest possible value of  $\beta_T$  in addition to maximizing the bootstrap fraction. Since  $\beta_p\beta_T = 25[(1+\kappa^2)/2](\beta_N/100)^2$ , where  $\kappa$  is plasma elongation, the requirements of steady-state operation and high fusion power density taken together make it necessary to operate near the pressure limit, with high  $\beta_N$  (Fig. 1).

Experiment and theory both show that these  $\beta$  limits are maximized by strong shaping (high triangularity and elongation) and broad pressure profiles [8–10].  $\beta$  is often limited in these experiments by an external kink mode in the presence of a resistive wall.

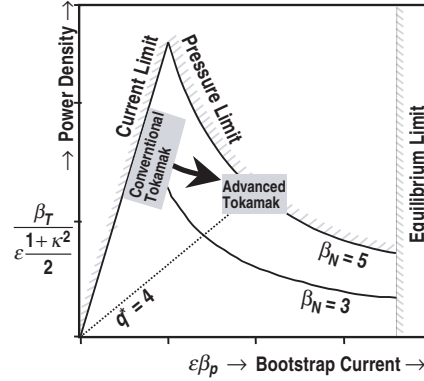


Fig. 1. Conventional tokamaks operate near the current limit, but Advanced Tokamaks operate near the pressure limit. The tradeoff between high bootstrap current and high power density makes it essential that the AT operate at high  $\beta_N$ .

This resistive wall mode (RWM) is stabilized in present experiments with toroidal rotation driven by tangential neutral beam injection (NBI), maintained with the aid of dynamic error field control [11]. Nonaxisymmetric coils recently installed inside the DIII-D vessel can be used to directly control the RWM, independently of rotation [12,13]. With the aid of these techniques, AT research in DIII-D is uniquely distinguished by operation above the no-wall beta limit. In transient experiments, the neoclassical tearing mode (NTM) often limits the duration of a high performance phase as a consequence of the evolution of the current profile. The NTM is expected to be stable with a properly chosen steady-state current profile. Stabilization of an otherwise unstable NTM has been demonstrated using localized ECCD injected into the magnetic island in several different devices [14–18].

Fusion gain increases with the triple product  $nT\tau_E \propto \beta_T \tau_E B^2$ . Therefore, maintaining high gain requires maximizing energy confinement, as well as  $\beta_T$ , especially at high  $\beta_p$  and lower  $I_p$ . This, along with the desire to gain some control over the kinetic profile shapes, motivates an effort to understand and control transport in these discharges. Although several tools have been identified that modify transport directly, the effect of the current profile on transport is large and remains an important, and perhaps dominant, transport control feature.

Finally, control of conditions at the boundary is critical for high performance experiments. In the near term, controlling the particle inventory in an AT discharge is important to maintain the density in a regime to obtain reactor relevant collisionality and for effective current drive. Divertor geometry must be consistent with particle control and shapes optimized for performance.

The basic requirements for the AT have been described in more detail previously [1,19,20]. In this paper, we will describe our approach toward developing AT scenarios at

DIII–D. In these plasmas, 15%–40% of the total current is provided by neutral beam current drive (NBCD), and about 10% by electron cyclotron current drive (ECCD), typically driven away from the magnetic axis at a point chosen by proper aiming of the antenna and selection of the value of  $B_T$ . Use of fast wave current drive (FWCD) is planned for future experiments and will be useful for controlling the central current density and electron temperature.

Our approach to AT development is described in Section II and Section III. In Section II, we report on focused studies in each of four scientific areas: MHD stability, transport physics, heating and current drive, and particle control. These efforts allow us to identify operational limits and to develop the means to expand them.

Simultaneous integration of the elements into steady-state high performance scenarios remains the greatest challenge. As we proceed through the discussion of the individual scientific elements of AT research, it will become clear that there are many interconnections between these elements. Developing the scientific understanding and needed control tools for increasing beta, controlling the current and pressure profiles and controlling the particle inventory poses challenges. Integration of these elements is discussed in Section III.

A comprehensive integrated modeling effort is being carried out in conjunction with these experimental efforts. Using both empirical and physics-based models, AT experiments are both planned and interpreted in light of these simulations. This effort benefits both the experiments and the models, since the results guide the development of both. This supports one of our major goals: To develop a predictive capability that can be applied to the design of advanced scenarios in next-step burning plasma experiments.

When applied to previously reported results [19,20], these simulations predicted we could produce fully noninductive discharges with higher  $\beta$  by increasing the heating power, primarily provided by NBI. Experimental efforts based on these projections have resulted in discharges which maintain a noninductive current fraction  $f_{NI} \approx 100\%$  for several confinement times, with  $\beta_N \leq 3.5$  and  $\beta_T \leq 3.6\%$ .

Many of the discharges with the highest noninductive current drive fraction tended toward lower confinement than discharges at lower  $f_{NI}$ . An understanding of this phenomenon is emerging, with ongoing studies of the effect of differing rotation and  $q$  profiles in different discharges. As our understanding of this issue improves, this may provide some insight into a method to improve control of future AT experiments in DIII–D.

Finally, these discussions will be summarized in Section IV.

## II. THE PHYSICS ELEMENTS OF ADVANCED TOKAMAK RESEARCH

Our approach to developing self-consistent integrated scenarios is to develop physics understanding and control capability of the individual scientific elements and then combine the knowledge and the tools to produce a steady-state high-performance scenario. We separate these elements into four general categories: Facilitating operation at high  $\beta$ , modifying and maintaining the current profile without inductive current drive, modifying and controlling transport, and modifying and controlling the particles and energy exhausted through the boundary. These are considered individually here; their use in integrated scenarios will be discussed in the following section.

The experiments described below all make use of variations on a typical DIII-D *AT* discharge. Evolution of such a discharge is shown in Fig. 2. Early in the current ramp, a momentary increase is programmed in the neutral beam power, triggering an early L–H transition. This broadens the temperature and density profiles and, by virtue of the addition of a pedestal, results in a high temperature core plasma, slowing the resistive evolution of the current profile and allowing access to plasmas with high  $q_{\min}$  after the plasma current has reached flattop. The high power phase is timed to coincide with the desired value of  $q_{\min}$ , typically 1.5–2.0 s for  $q_{\min} \geq 2.5$  and 2.5–3.0 s for  $q_{\min} \geq 1.5$ . The shape of these plasmas conforms with the pumped divertor, which is presently designed to allow density control in moderately shaped (triangularity at the pumped end of the plasma  $\delta_x \approx 0.65$ , typical triangularity at the opposite end of these plasmas is  $\delta_r \approx 0.3$ ) single-null divertor plasmas.

### A. High beta operation

Simultaneously optimizing both fusion power density ( $\beta_T$ ) and bootstrap fraction ( $\beta_p$ ) drives us to operate near the pressure limit (Fig. 1), with high  $\beta_N$ . Present *AT* experiments in DIII-D operate in the range  $\beta_N \approx 3$ –4, and we anticipate increased values in the future. In order to reach these values, the plasmas must be optimized for high magnetohydrodynamic (MHD) stability. We concentrate on several areas: the geometry and the pressure profile shape, stabilization of the RWM and either avoidance or stabilization of the NTM.

Strong shaping and a broad pressure profile are both favorable for increasing the stability limit [Fig. 3(a)] [8]. Recent modeling using geometry and pressure profiles (including the H-mode pedestal) relevant to DIII-D *AT* experiments [9,10] demonstrate

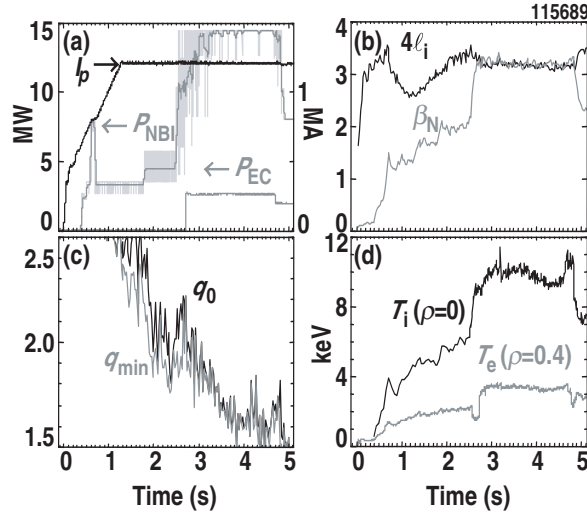


Fig. 2. A typical AT discharge with  $f_{NI} \approx 100\%$ ,  $\beta_N \approx 3.1$  and  $\beta_T \approx 3.2\%$ . Current profile evolution continues after the application of ECCD, but eventually ceases and the plasma state remains stationary until the end of the ECCD pulse. (a) Plasma current  $I_p$ , neutral beam power  $P_{NBI}$ , EC power  $P_{EC}$ ; (b) normalized beta  $\beta_N$ , approximate no-wall beta limit  $4\ell_i$ ; (c) axial ( $q_0$ ) and minimum ( $q_{min}$ ) safety factors; (d) ion temperature  $T_i$  at the magnetic axis and electron temperature  $T_e$  at the EC deposition location ( $\rho = 0.4$ ).

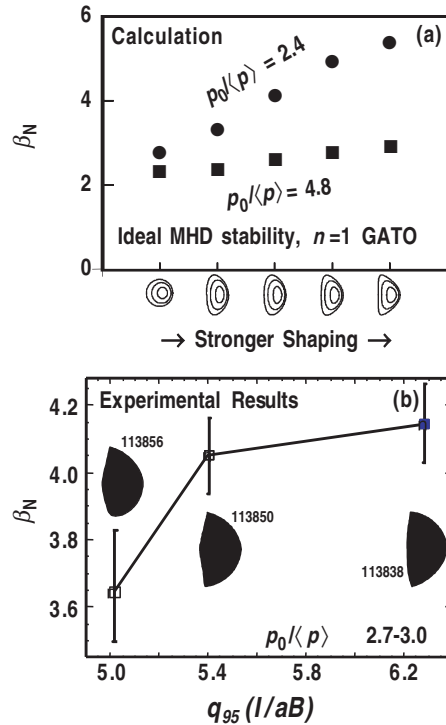


Fig. 3. Both theory (a) and experiment (b) show that  $\beta$  limits are maximized with strong shaping, characterized by an increasing “shape parameter”  $S = q_{95} (I/aB) \sim a/R (1 + \kappa^2/2) [1+3/2 (a/R)^2 \dots] f(\delta, \dots)$ . ..  $S$  increases with increasing shaping (elongation, triangularity, ...) and has previously been associated with high  $\beta$  stability [22].

that increases in triangularity and elongation increase the ideal, low- $n$   $\beta_N$  limits that often limit performance in *AT* discharges.

An experiment to test the dependence on geometry was carried out, in which the shape was changed adiabatically from 1.5-2.5 s (to maintain identical current ramp phases for all discharges). The divertor cryopump was not used, since the stronger shaping in some of these discharges was done at the expense of optimum positioning of the strike point for particle control. This results in higher densities and broader profiles, but this effect is uniform over the variation of shapes. After changing the shape, the heating power was increased to  $P_{\text{NBI}} = 15$  MW, with  $\beta_N$  increasing to above 3.5. The single-null (elongation  $\kappa = 1.76$ , up/down average triangularity  $\delta_{\text{ave}} = 0.45$ ) discharge disrupted with  $\beta_N \approx 3.6$  due to a fast growing  $n = 1$  mode. Two double-null discharges, one with  $\kappa = 1.86$ ,  $\delta_{\text{ave}} = 0.50$  and the other with  $\kappa = 1.94$ ,  $\delta_{\text{ave}} = 0.64$ , continued to higher  $\beta_N$ , after which their performance degraded somewhat due to edge localized modes (ELMs), but with no disruptive instability (Fig. 3). These experiments, consistent with the calculations, indicate an advantage not only to stronger shaping, but in adding a second X-point and operating a double- rather than single-null configuration.

Another important factor in MHD stability is the shape of the pressure profile. Both theoretical studies [8,9] and operating experience on DIII-D indicate that high  $\beta$  stability to low- $n$  instabilities is improved with a broader pressure profile. An experiment was carried out to test this specifically for *AT* plasmas. The early evolution of these plasmas was essentially the same as shown in Fig. 2, but the high power phase started at 1.5 s in order to operate with high  $q_{\text{min}} > 2$ . Previous experiments and calculations [23] found that  $\beta$  limits were lower in this regime, and there was some consideration given to the possibility that these plasmas might be more sensitive to pressure profile peaking. In some of these discharges, gas was puffed into the plasma simultaneous with the high power phase, thereby broadening the density profile, and in turn, the pressure profile (Fig. 4).

A discharge without this gas puff disrupted with  $\beta_N \approx 3.4$ , due to an  $n = 1$  RWM. The pressure peaking factor  $p(O)/\langle p \rangle$  was 2.8 in this case. A similar plasma with the gas puff had  $p(O)/\langle p \rangle \approx 2.2$  at the same time as the disruption in the first discharge. At this time, the plasma with a broader pressure profile had reached  $\beta_N \approx 3.8$ , and subsequently increased to  $\beta_N \approx 4$  without encountering an RWM or global kink mode. In this case  $\beta$  was limited by bursts of tearing modes.

Consistent with calculations, we found that low- $n$   $\beta$  limits could be substantially increased by stronger plasma shaping and broadening of the pressure profile. One key motivation for increasing  $\beta_N$  is the resultant increase in bootstrap fraction and reduced current drive requirements. However, both of these experiments achieved these

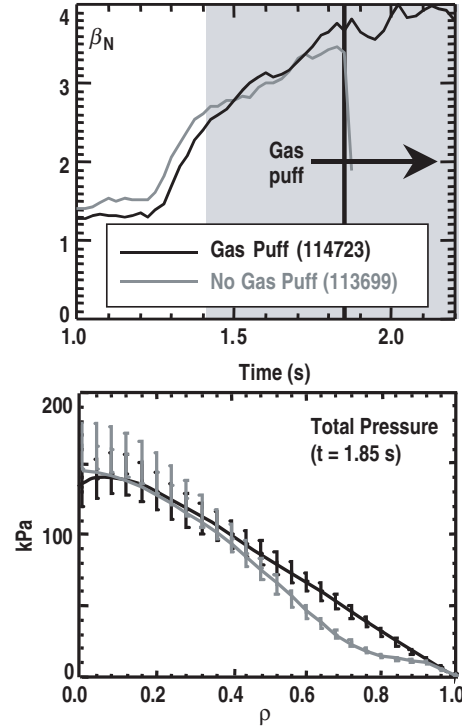


Fig. 4. An *AT* discharge (no ECCD) disrupts at  $\beta_N \approx 3.4$  with a pressure peaking factor  $p(0)/\langle p \rangle \approx 2.8$  (grey). In a similar discharge (black), gas puffing is deployed to broaden the density and pressure profiles so that  $p(0)/\langle p \rangle \approx 2.2$ , resulting in  $\beta_N$  reaching 4.

conditions using a technique that resulted in increased density, either by moving the plasma away from the divertor cryopump or by puffing gas into the vessel. This is in conflict with the requirement of density control to allow effective external current drive. This requirement, and steps planned to address it consistent with these stability considerations, are described in Section II.D. These optimizations also allow increasing  $\beta$  to levels where neoclassical tearing modes (NTM) and resistive wall modes (RWM) limit performance.

NTMs often appear in *AT* and other plasmas as the  $q$  profile evolves through low-order rational values. These can severely limit performance.  $m/n = 3/2$  and  $2/1$  NTMs have successfully been stabilized by driving current with electron cyclotron waves (ECCD) in the magnetic island [1418], typically very far from the magnetic axis ( $\rho \approx 0.7$ ). This technique allows continued high  $\beta$  operation.

Steady-state high bootstrap fraction *AT* discharges are designed to operate with stationary  $q$  profiles that can avoid unstable low-order rational  $q$  surfaces and thus avoid NTMs. An example is shown in Fig. 5: Two similar *AT* plasmas are compared, one with and one without ECCD. In the discharge without ECCD, the current profile continues to evolve with  $\beta_N \approx 3$ , until magnetic probes indicate the appearance of an instability at

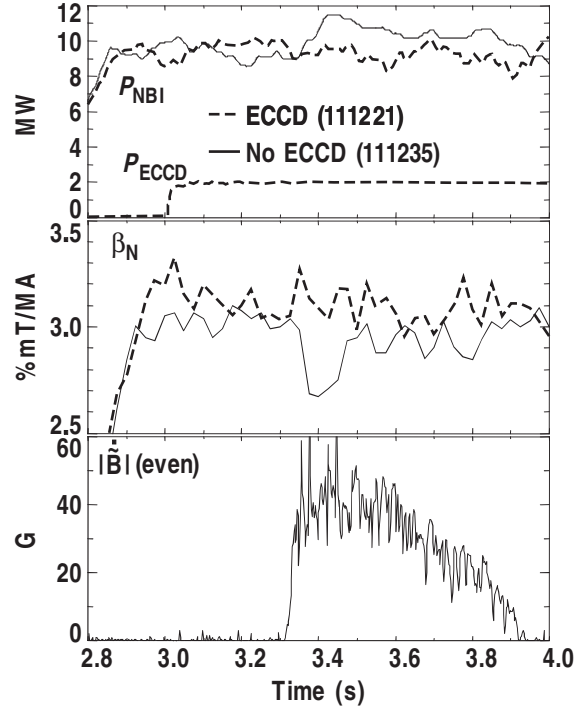


Fig. 5. A comparison of AT discharges with and without ECCD. Without ECCD (solid), an NTM eventually appears as the  $q$  profile evolves, and degrades confinement. The mode eventually disappears as the  $q$  profile continues to change. With off-axis ECCD (dashed,  $P_{\text{EC}} \approx 2.5$  MW,  $\rho_{\text{EC}} \approx 0.4$ ), the  $q$  profile evolution is slowed so that the mode does not appear.

3.3 s. Coincident with this,  $\beta_N$  decreases, and neutral beam heating power demand increases (the plasma control system is adjusting power in an attempt to keep the stored energy fixed), indicating degraded confinement. This continues throughout the duration of the elevated MHD signal, which later terminates as the  $q$  profile continues to evolve. In the other discharge, approximately 2 MW of ECCD is injected at  $\rho \approx 0.4$  starting at 3.0 s. The ECCD maintains  $q_{\text{min}} > 2$  so that the NTM never becomes unstable. The MHD does not appear in this discharge, indicating that the current profile modification stemming from the ECCD is preventing the mode from occurring.

AT plasmas in DIII-D routinely operate above the no-wall limit. This is made possible by rotational stabilization of the RWM, which is in turn facilitated by active control of error fields in the tokamak that might otherwise cause the toroidal rotation to slow. Coils have recently been installed inside the DIII-D vessel which are designed to provide direct stabilization of the RWM in the absence of toroidal rotation. Efforts to exploit these coils in experiments have begun, with the detailed results being described in other papers [12,13,24].

## B. Maintaining the current profile without inductive drive

In conventional tokamak scenarios, most of the current is driven by inductive means, with the plasma acting as the secondary of a transformer. This makes such scenarios inherently pulsed, thereby decreasing the average power output from a power plant and resulting in both thermal and mechanical stresses on many components of the device. At the core of the *AT* concept is elimination of this pulsed requirement, allowing for steady state operation of a tokamak without sacrificing fusion performance.

For steady-state operation, the plasma current must be provided by means other than transformer action. The cost and power consumption associated with providing a large part of this current by external means could be prohibitive. The bootstrap current [7] can be used to provide most of the current in high  $\beta$  steady-state plasmas. This current is driven by radial gradients of the kinetic profiles by the plasma itself.

In a global sense, the bootstrap fraction  $f_{BS} \propto \beta_p \propto q\beta_N$ . Optimizing  $f_{BS}$  requires operation at maximum  $\beta$  at modest values of the safety factor  $q$  (Fig. 1). There have been experimental observations indicating degraded MHD stability at higher values of  $q$  [23], so there are tradeoffs that must be taken into account. Maximizing the total amount of bootstrap current is not sufficient, though. Locally, the current depends directly on the kinetic profiles, and can be written as  $j_{BS} = C_n (\nabla n/n) + C_{Te} (\nabla T_e/T_e) + C_{Ti} (\nabla T_i/T_i)$ . The desired broad bootstrap current density profile would then be associated with a broad pressure profile (already identified as favorable for MHD stability). More specifically, since the largest of these coefficients would be  $C_n$  in both a reactor and in DIII-D, a broad density profile is desirable.

*AT* discharges in DIII-D typically have  $f_{BS} = 50\%–70\%$ , and simulations indicate that scenarios are feasible with  $f_{BS} > 90\%$ . The highest bootstrap fraction scenarios would require reduction or elimination of the NBCD, which provides 15%–40% of the total current in present experiments. In DIII-D *AT* target plasmas (prior to the introduction of ECCD), the remaining inductive current in the plasma amounts to about 25% of the total current, and is centered around the mid radius (Fig. 6) [1]. It is this portion of the total current that must be replaced by additional noninductive sources in order to reach steady state.

Electron cyclotron current drive is being developed as an effective tool to provide this off-axis current in DIII-D. The behavior of this tool is well understood and is accurately predicted [25] by modeling. Figure 7 shows results of a recent experiment where 2 MW of EC power was applied at  $\rho \approx 0.4$  [21]. Simulation of a discharge with and one without EC indicate a difference in current density at the location where the EC waves are

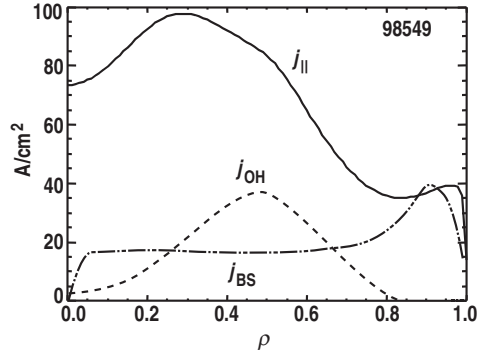


Fig. 6. Results from an *AT* discharge with  $f_{BS} \approx 50\%$  and  $f_{NBI} \approx 25\%$  and no ECCD. Under these conditions,  $f_{Ohmic} \approx 25\%$ , all centered around the mid radius. Reaching steady state is expected to be possible by applying ECCD in this region. Without doing so, this discharge would eventually evolve so that the inductive current penetrates to the axis [1].

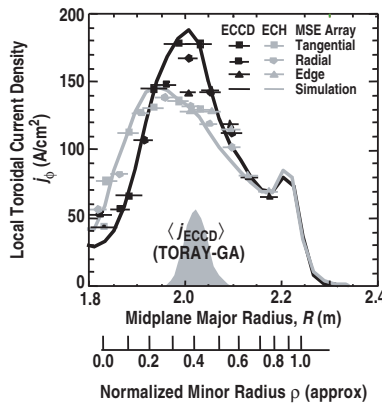


Fig. 7. First demonstration of  $j(\rho)$  control using ECCD in a DIII-D *AT* plasma, with  $P_{EC} \approx 2.5$  MW driving about 130 kA of current. Simulations and measurement are in good agreement for two discharges, one with (ECCD) current drive and the other where the EC waves are aimed to heat without current drive (ECH), and indicate that the strength and location of this driven current are in keeping with expectations. The horizontal bars in the figure indicate the spatial extent sampled by each MSE channel.

deposited. Measurements, made by motional Stark effect (MSE) [26], are in good agreement with the simulation, and indicate that approximately 130 kA is driven by ECCD near the absorption radius.

As will be shown in Section III, fully noninductive discharges are attainable using bootstrap, NBCD and ECCD. However, both experimental experience and simulations indicate that the plasma response to off-axis ECCD often includes an increase in  $q_0$ , the safety factor in the vicinity of the axis, due to the induced electromotive force opposing the driven current (back-EMF).

The back-EMF has two important implications: First, the plasma can undergo a long evolution before reaching steady state. Second, that steady state would have strong

negative shear in the core, likely inducing an internal transport barrier (Section II.C.) in several or all transport channels [27]. Calculations and experiment indicate a transport barrier at small minor radius leads to a reduced  $\beta$  limit as a consequence of pressure profile peaking. Another source of current, near the magnetic axis, is desirable to control this magnetic shear. Model calculations indicate that FWCD or additional ECCD would be effective for supplying the needed axial current. FWCD would have the added benefit of increasing both  $T_e$  and  $\beta_e$ , and consequently increasing the off-axis current driven by ECCD. The fast wave system on DIII-D is currently being restarted after several years without operation. Fast wave experiments have begun, with initial results indicating behavior consistent with these long-term goals [28].

### C. Transport considerations

Advanced Tokamaks are characterized by high fusion gain (high  $\beta\tau$ , the product of the plasma beta and confinement time) and duty factor approaching 100% (steady-state, facilitated by high  $f_{BS}$ ). Based on the above discussions of MHD stability and current profile control, both of these goals are facilitated by a broad pressure profile. It is desirable, then, to gain some measure of control over the kinetic profiles.

The profiles are largely determined by sources and transport. In DIII-D, NBI, electron cyclotron (ECH) and fast wave (FWH) heating are all sources of energy. NBI and gas puffing (primarily early in the discharge) provide particle sources. Our ability to control the deposition of these sources is limited and will become more difficult in a future burning plasma, where the main heat source will be provided by fusion alpha particles.

The present understanding of transport [29,30] is that it is mainly driven by turbulence on several different scale lengths. We have identified suppression mechanisms that are believed to act on each of these.  $\mathbf{E} \times \mathbf{B}$  shear [31] can limit the longer wavelength turbulence, especially the ion temperature gradient (ITG) mode, and is believed responsible for much of the physics associated with internal transport barriers appearing in the ion channel in DIII-D [32].  $\alpha$ -stabilization, also referred to as Shafranov shift stabilization, [33,34] is associated with transport reductions across a wider range of scale lengths and in all transport channels. Negative magnetic shear, as exists in the core of DIII-D AT plasmas, is also stabilizing, and works in concert with  $\alpha$ -stabilization [33]. Transport barriers appearing in the electron channel under conditions of intense electron heating are believed to be associated with  $\alpha$ -stabilization [35].

We anticipate that the largest impact on transport in a burning plasma device will come not from direct manipulation of transport, but through changes made to other plasma parameters. This is especially true of the current profile, since we anticipate the

largest external power source in such devices will be the current profile control tool. This presents a challenge to the development of integrated *AT* scenarios: Without independent control of the current profile and transport, we must search for self-consistent solutions (see Section III) possessing the desirable characteristics. Some measure of independent control of these parameters would allow for greatly improved flexibility.

For example, as previously mentioned, application of off-axis ECCD to *AT* plasmas can result in strongly negative magnetic shear. In the case shown in Fig. 8, this magnetic shear was sufficient to trigger formation of an internal transport barrier (ITB). This in turn results in decreased MHD stability at high beta and a narrowing of the bootstrap current profile.

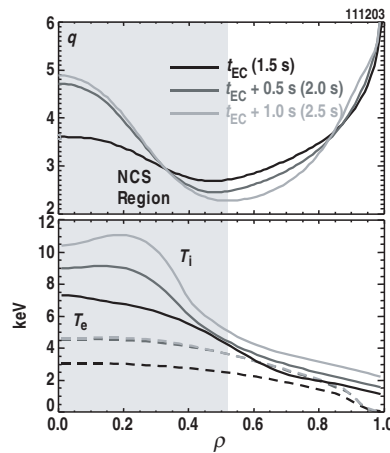


Fig. 8. ECCD driven current at  $\rho \approx 0.4$  results in changes to the entire current profile, and sharp increases in  $q_0$ . The resulting negative shear can trigger the formation of an internal transport barrier, thus demonstrating the impact that current profile modification has on transport and the kinetic profiles.

We do have the ability to control transport in a limited fashion. A number of tools have been identified on DIII-D as having impact here.  $\mathbf{E} \times \mathbf{B}$  shear can be driven or modified by NBI. Pellet injection [36] and rf [37] have also both been used to modify this shear. Studies of these and their effects on transport will continue, with more flexibility becoming available with the planned future reversal of one beamline (two NBI sources, out of a total of eight). This will allow a large range of variation in the strength and characteristics of this shear, the nature of which differs depending on the direction of the beam injection [32].

Both NBI and pellets also affect  $\alpha$ -stabilization, as do ECH/ECCD and FWH/FWCD. Impurity injection and particle removal via divertor cryopumping also have direct impact on transport.

It is likely in a future device, however, that the dominant external influence on transport will be provided through control of the current profile. This underscores the importance of sufficient understanding of the physics involved so that these regimes can be simultaneously optimized for MHD stability, current profile control and transport.

#### D. Boundary control

The fourth area to be considered is the plasma boundary, namely handling the particles and energy that flow through the boundary. In a power plant, heat removal is a key issue, especially in *AT* scenarios at higher power densities. Boundary control plays an additional important role in DIII-D. As we have shown, controlling the current profile is a key element in achieving steady-state operation with high  $\beta$  and good confinement. The divertor provides density control to maintain the effectiveness of the current drive tool at reactor relevant collisionality.

ECCD driven current scales as  $T_e/(n_e R)\beta_e^{1/2}$  [38], so that driven current decreases with increasing density. Furthermore, EC waves do not penetrate the plasma above a cutoff density, about  $6 \times 10^{19} \text{ m}^{-3}$  in typical DIII-D *AT* plasmas. Present experiments are carried out in a single-null geometry, with  $\delta \approx 0.65$  at the pumped end of the plasma (usually much lower at the opposite end). This geometry is chosen to match the divertor, which has cryopumps coupled to both divertor legs of this configuration. Density is well controlled in these plasmas, in the range  $\langle n_e \rangle \approx 3\text{--}4 \times 10^{19} \text{ m}^{-3}$ .

As previously discussed, further optimization of *AT* performance can be gained with more strongly shaped plasmas, with higher elongation and triangularity, as well as a double-null divertor configuration. An experiment was performed to evaluate pumping requirements for plasmas moving away from the optimal (for density control) shape [39]. With the standard shape, conforming to the pumped divertor, steady discharges were produced in several shapes, ranging from the standard upper single-null *AT* shape to a similar, but inverted, lower single-null (Fig. 9). The fraction of particles removed,  $\Gamma_{\text{OUT}}/\Gamma_{\text{INJ}} + \Gamma_{\text{IN}}/\Gamma_{\text{INJ}}$  ( $\Gamma_{\text{OUT}}$  is the particle flux into the pump at the outer strike point,  $\Gamma_{\text{IN}}$  is the flux to the inner pump and  $\Gamma_{\text{INJ}}$  is the source particle flux, arising from NBI) ranges from nearly 100% for an upper single-null to only about 50% for the inverted plasma. About 65% of the particles are removed from the double-null plasma.

In a related experiment, *AT* discharges were produced in the double-null shape. Although high performance was obtained in these discharges, the lowest sustainable density achieved was near the EC cutoff, limiting the use of ECCD in these discharges. The desire for the improved performance associated with stronger shaping, coupled with the need for effective density control, motivates our plan to add a pumped divertor at the bottom of the vessel.

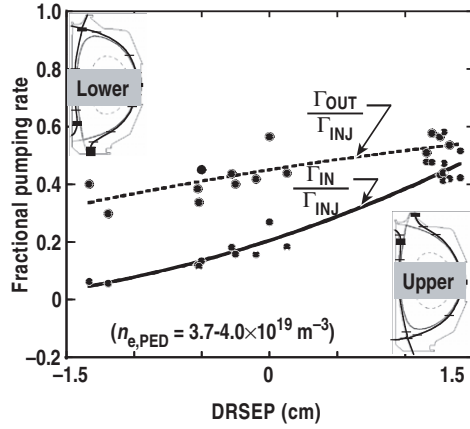


Fig. 9. Fractional pumping rates for the inner ( $\Gamma_{IN}/\Gamma_{INJ}$ ) and outer ( $\Gamma_{OUT}/\Gamma_{INJ}$ ) divertor cryopumps.  $\Gamma_{INJ}$  is the rate at which the plasma is fueled by neutral beams (the only significant fueling source in *AT* plasmas in DIII-D). To maintain a constant density, the sum of the two curves should approach 100%, and this is the case for an upper single-null divertor plasma with both strike points coupled to pumps. As the magnetic balance, indicated by DRSEP, is shifted from upper, through double-null (DRSEP = 0) to lower single-null, the pumping rates are decreased to about 50% for the DRSEP = -1.5 cm case. This data indicates that density control in a double-null divertor configuration will require pumps at both ends of the plasma.

### III. INTEGRATED SELF-CONSISTENT SCENARIOS

In developing *AT* regimes, the key challenge is to combine the important elements in an integrated fashion. In this section, we will briefly discuss two efforts that aid in this integration, and present some recent results in the development of high performance integrated scenarios with  $f_{\text{NI}} \approx 100\%$ .

#### A. Plasma control system

The DIII-D Plasma Control System (PCS) [40] controls many of the tokamak's global parameters, including shape, plasma current and stored energy. The special requirements of the *AT* demand additional control, in particular, of *profiles* rather than only global parameters.

We have discussed a number of tools that can be employed to directly control or indirectly influence profile quantities. We have begun efforts to use the PCS to control some of these in real time. Single point control has been used, with an electron cyclotron emission (ECE) measurement as the sensor and ECH (aimed at the same location in the plasma) as the actuator to finely control the evolution of the electron temperature during the current ramp at the beginning of an *AT* discharge [41]. This technique allowed improved reliability and reproducibility in producing an *AT* target, since the current profile during this part of the discharge is determined strongly by  $T_e$  through its impact on resistivity.

This capability will be expanded to perform multi-point control of  $T_e(\rho, t)$  and other profiles.  $q(\rho, t)$  profiles are already being analyzed in real-time, using MSE data and the rtEFIT (real-time EFIT) [42] code. This sensor, combined with ECCD and FWCD as actuators, will be used in the very near future to develop real-time current profile control.

#### B. Integrated modeling

Modeling and simulation have become essential tools for both experimental interpretation and planning. Predictive modeling is used to plan *AT* experiments, based both on empirical extensions from previous experiments and theoretical models [19]. The experiments are also interpreted through the use of these models, with the results being used not only to plan further experiments, but in continued development of the models themselves. This approach not only contributes to progress in the experimental effort, but

to the ultimate goal of developing a fully predictive capability that can be applied beyond DIII-D, to design advanced regimes for next-step burning plasma devices.

Such predictive modeling was carried out based on previously reported discharges [19] using transport coefficients determined from power balance analysis of experimental discharges and scaled by the IPB98(y,2) H-mode confinement scaling relation [43] (Fig. 10). IPB98(y,2) is pessimistic in its power dependence, so these calculations were expected to be quite conservative in their predicted power requirements. The discharge that formed the basis of this study has been reported on previously [19] and had  $q_{\min} > 1.5$ ,  $\beta_N^{\max} \approx 3.1$ ,  $f_{BS} \approx 55\%$  and  $f_{NI} \approx 90\%$ . The simulations indicate that increasing the neutral beam power, from 9 to 13 MW, would result in the plasma reaching  $f_{NI} \approx 100\%$  at somewhat higher  $\beta$ . The same calculations were repeated using the theory-based GLF23 model [44], with the results being consistent with the empirical prediction.

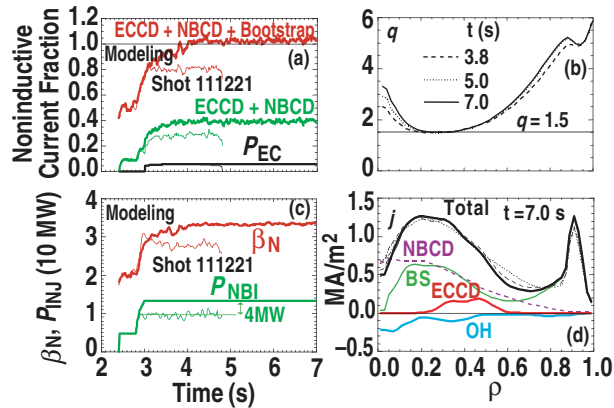


Fig. 10. (a) Noninductive current fractions from ECCD+NBCD (green) and total including bootstrap (red) for experimental (with  $f_{NI} \approx 90\%$ , thin lines) and simulated ( $f_{NI} \approx 100\%$ , thick) discharges. The waveform shown for the ECCD indicates that no increase in EC power is required. (b)  $q$  profiles at several times during the simulation indicating a slow continued evolution of  $q$  at the magnetic axis, but  $q_{\min}$  remains constant. (c) Both  $\beta_N$  (red) and neutral beam power (green) are increased in the simulation. (d) Total current profile (black) shown at the same times as in (b) and the components of this current at the end of the simulation (color). The slow evolution previously noted in  $q_0$  is due to a small remaining inductive counter-current near the axis; this back-EMF gradually relaxes given sufficient time.

More recently, the renormalized GLF23 model was used to perform steady-state calculations of an AT discharge. The model now reproduces the measured profiles well in discharges with  $H_{89} \approx 2.3$  (Fig. 11). In the region of the plasma surrounding the magnetic axis (inside  $\rho \approx 0.2-0.3$ ), the gradients fall below the critical level and transport is predicted to be neoclassical. Here, a multiplier is applied to the neoclassical prediction. Although this multiplier is determined empirically, the same multiplier appears to work well in all high confinement ( $H_{89} \approx 2.3$ ) AT discharges. Note that in contrast to previous GLF23 simulations, the density profile is now being evolved, with the results bearing a

strong resemblance to the experimental data. In all profiles, however, a boundary condition is imposed at  $\rho = 0.8$ , so that the pedestal is still not calculated.

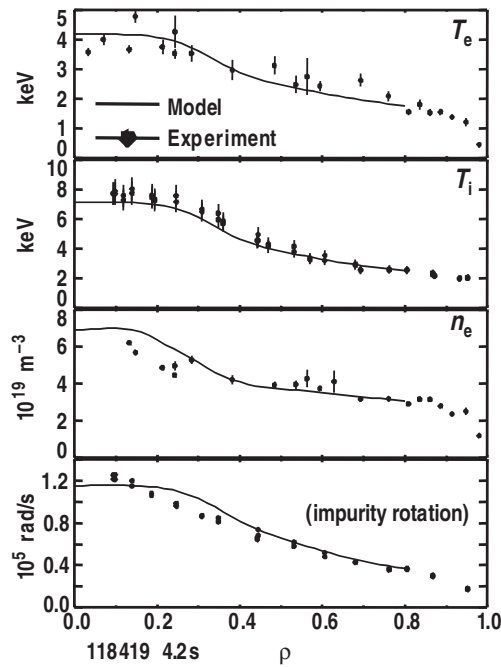


Fig. 11. Results from a steady-state simulation of an AT discharge with GLF23. Density, temperature and toroidal rotation velocity are all evolved. Shot 118419:  $I_p = 1.1$  MA,  $B_T = 1.7$  T,  $H_{99} = 2.3$ ,  $\beta_N = 3.3$ ,  $P_{\text{NBI}} = 8.9$  MW.

### C. Recent progress in integrated scenario experiments in DIII-D

Experiments have now been carried out to test these predictions [45]. Target discharges similar to the previous experiments, with  $q_{\text{min}} > 1.5$ , are prepared in the same way, with an early H-mode transition being used to slow the current profile evolution. Several discharges were run, with varying levels of NBI power, resulting in  $f_{\text{NI}} \approx 100\%$  being maintained for up to 1 s with  $\beta_N$  up to 3.5 ( $\beta_T$  up to 3.6%). A time history of one of these discharges, with  $\beta_N \approx 3.2$  and  $H_{99} \approx 1.9$  is shown in Fig. 2. Note that for most of these discharges,  $\beta_N$  is maintained at a level slightly above the no-wall stability limit. As will be shown below, it should also be noted that although these discharges globally reach  $f_{\text{NI}} \approx 100\%$ , the locally calculated inductive current does not fully relax to zero.

The makeup of the current profile in these discharges was analyzed using three different codes: ONETWO [46] and TRANSP [47] are both transport codes. In these calculations, the bootstrap current is determined using models (NCLASS [48] or Sauter [49]). Neutral beam driven current is calculated using models internal to the codes. ECCD is calculated using TORAY-GA [50]. The inductive current density is then

determined by subtracting these calculated noninductive currents from the total current calculated from a reconstruction of the plasma equilibrium using EFIT [51].

An alternate method of calculating the inductive current density profile uses the NVLOOP code [52]. The poloidal flux,  $\Psi(\rho, t)$  is given by a series of equilibrium reconstructions with a fine time resolution based on the MSE diagnostic and magnetic measurements incorporated with pressure profiles. The total current is given by spatial derivatives of  $\Psi$ , while the inductive current  $j_{OH}$  is given by  $\sigma_{neo} E_{||}$ , where  $\sigma_{neo}$  is the neoclassical conductivity and  $E_{||}$  is the parallel electric field determined by the time derivative of  $\Psi$ . The noninductive current can be calculated by subtracting the calculated inductive current from the total current, and can be compared with the sum of ECCD, NBCD and bootstrap currents as described above.

Figure 12 shows results of such calculations from TRANSP (using the Sauter bootstrap formulation) and NVLOOP for the discharge shown in Fig. 2. The other calculations described above give similar results. Figure 12(a) shows the noninductive current fraction  $f_{NI} = I_{NI}/I_{total}$  and indicates that this discharge is nearly 100% noninductively sustained for over 0.5 s. A snapshot of the different components of the current near the end of the ECCD pulse is shown in Fig. 12(b), indicating that although the net current (integrated over the cross section of the plasma) is nearly 100% noninductive, locally, this is not so.

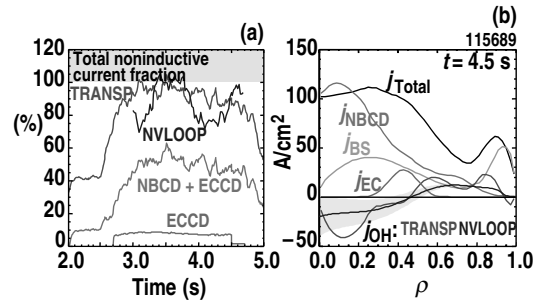


Fig. 12. A discharge reaches net noninductive conditions with off-axis ECCD, which can be maintained for over 0.5 s. Near the axis of these plasmas, neutral beam current drive actually overdrives the total current, resulting in inductive counter-current to balance the noninductive sources. Decreasing the neutral beam power and increasing the duration is anticipated to allow further relaxation of the inductive current to zero.

Although the inductive current is not fully relaxed to zero across the profile in these discharges, the current profile does become nearly stationary for about one current relaxation time ( $\approx 1.1$  s; Fig. 13). The target discharges in the present experiments have monotonic  $q$  profiles, contrasting with previous experiments where the target  $q$  profile had negative central shear (NCS). Since the final, stationary, configurations do have some amount of NCS, the period of evolution required to reach this final state is longer in these experiments. This is a consequence of irreproducibility in the startup phase, since

the intent is to prepare a target plasma that already has close to the desired current profile, so that ECCD only has to maintain rather than develop the final state. After 0.7 seconds, little further evolution takes place for the duration of the ECCD pulse.

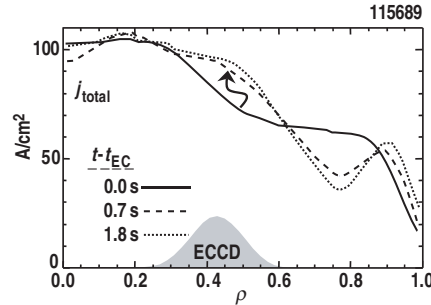


Fig. 13. The profiles undergo significant evolution following introduction of ECCD, taking about 0.7 s to reach equilibrium. The current profile becomes nearly stationary after this time.

In these experiments, the neutral beam power is feedback controlled to maintain  $\beta_N$  at a particular value, usually close to the stability limit. Thus, the required heating power is determined by a combination of MHD stability and confinement, with a lower confinement discharge requiring more power from NBI. In order to reach and maintain  $f_{NI} \approx 100\%$ , both globally and locally, a certain amount of NBCD is needed, which often will be different than the amount determined as described above. The discharges with  $f_{NI} \approx 100\%$  had a higher power demand (lower confinement,  $H_{89} \approx 1.9$  instead of  $H_{89} \approx 2.3-2.4$ ) than the previous discharges, and so  $j(\rho)$  in the region surrounding the magnetic axis is overdriven by NBCD (Fig. 12). The inductive current density, counter to the total current, is a consequence of this NBCD overdrive.

This points out the need for a mechanism that can independently control transport. Since we have already demonstrated discharges with too high and too low an NBI power demand, understanding of the mechanism behind these confinement differences may lead to a tool that could potentially allow us to select  $P_{NBI}$  for the right amount of NBCD to eliminate the inductive current. We would then seek to adjust transport accordingly.

Studies are underway to determine this mechanism. A comparison of profiles in two discharges representing the high and low confinement conditions is shown in Fig. 14 (note that the lower confinement discharge has 60% higher neutral beam power and 9% higher plasma current and toroidal field). Two candidates emerge as possible causes for the change in confinement: differences in the  $q$  profile and in the rotation profile.

Examination of a set of similar discharges including examples of both the “high” and “low” confinement conditions indicates that reversal of the  $q$  profile is probably not the controlling factor, as there is no clear variation of  $H_{89}$  vs.  $q_0 - q_{min}$ . The presence of a

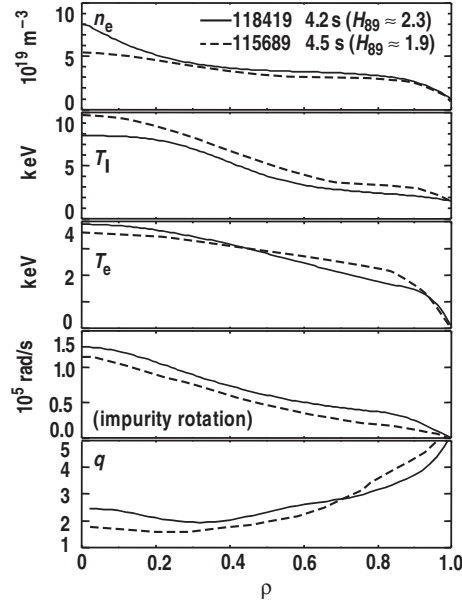


Fig. 14. Profiles of two similar AT discharges with differing confinement. Significant differences are seen in the toroidal rotation and  $q$  profile. 115689:  $I_p = 1.2$  MA,  $B_T = 1.85$  T,  $H_{89} = 1.9$ ,  $\beta_N = 3.2$ ,  $P_{\text{NBI}} = 14.5$  MW. 118419:  $I_p = 1.1$  MA,  $B_T = 1.7$  T,  $H_{89} = 2.3$ ,  $\beta_N = 3.3$ ,  $P_{\text{NBI}} = 8.9$  MW.

$q = 2$  surface was also considered, but there are examples of discharges with  $H_{89} \approx 2.3$  with  $q_{\text{min}} < 2$ .

At present, we believe the important difference is that seen in the toroidal rotation. The pedestal in the rotation profile is eliminated in the lower confinement discharges, and the reduced rotation propagates all the way into the center of the discharge. Both the shear in toroidal rotation and the value of rotation velocity are known to play important roles in determining transport, so this is not surprising. Both the cause of the reduced rotation and its effect on transport remain under investigation. A possible cause for this change in rotation has been identified, and will be the subject of an upcoming experiment. If we can verify that this is the cause, it may present an opportunity to improve control over confinement in AT regimes in DIII-D, thereby allowing us to at least in some measure decouple beta and NBCD.

Since DIII-D AT discharges typically operate in the regime where transport is subcritical (reduced but not completely suppressed) to  $E \times B$  shear, we can speculate that transport can be continuously varied by varying the rotation and therefore the  $E \times B$  shearing rate. Although a burning plasma device may not exhibit significant toroidal rotation,  $E \times B$  shear should still be an important effect through the effect of the pressure gradient term in the force balance equation determining  $E_r$  [32,53,54]. Similar opportunities for control may therefore present themselves in ITER AT discharges, although the details of the control mechanism may be substantially different.

## IV. SUMMARY AND FUTURE WORK

Advanced Tokamak research in DIII-D seeks to provide a scientific basis for operating steady state high performance regimes in next-step tokamaks. Our approach is to develop understanding of the key elements as well as the tools, separately or in concert, and then integrate these elements into self-consistent discharges exhibiting most or all of the features desired in an *AT*. The experimental effort is guided by integrated modeling, which benefits not only the immediate experimental goals, but also fosters longer term development of a capability to predict performance in a next-step device with burning plasma.

The control tools fall into four broad categories: tools to increase  $\beta$ , tools to control the current profile, tools to control the kinetic profiles through transport and tools to control the particles and energy exhausted from the plasma. The  $\beta$  limit is maximized through strong shaping and broad pressure profiles. Operation above the no-wall  $\beta$  limit is made possible by stabilization of the resistive wall mode, either through rotation or directly with nonaxisymmetric coils. Most of the current in these plasmas will be driven by bootstrap, which is optimized with a broad pressure profile and high  $q$ . The remaining current is provided by externally driven noninductive means. In DIII-D, these include NBCD and FWCD (centered on the axis) and off-axis ECCD. The required broad pressure profiles would be facilitated by some control of transport. The most powerful actuator for transport, however, is through the current profile. Modification of rotation and  $E \times B$  shear may allow some additional transport control. Another important factor determining the current profile is the density profile. Divertor cryopumps have demonstrated their capability of maintaining constant and reasonably low density. Optimization of the shape for MHD stability may, however, require some modification of the divertor geometry. In DIII-D, a double-null pumped divertor is being planned for this purpose.

Integration of these distinct elements occurs through the use of a sophisticated plasma control system and an extensive integrated modeling effort. The DIII-D plasma control system is being continuously developed toward the ability to control profiles in real-time, in addition to global parameters. Integrated modeling is used both to design experiments and to interpret their results. The modeling uses both empirical and theory-based models, and the comparisons with experimental results are particularly useful in the further development of the models. Although this approach has been very successful in devising experiments, its biggest value may lie in the ever improving predictive capability driven

by this effort. The same tools being applied to experimental design and interpretation on DIII-D are already being applied to simulations of burning plasma devices.

Based on previous results, simulations predicted that fully noninductive discharges could be produced in DIII-D with similar parameters, but with increased heating power. Experiments following this prescription resulted in plasmas with  $f_{\text{NI}} \approx 100\%$ ,  $\beta_{\text{N}} \leq 3.5\%$ -m-T/MA and  $\beta_{\text{T}} \leq 3.6\%$ . Although the net inductive current in these discharges approaches zero, the local inductive current density remains finite. Near the magnetic axis, the neutral beam drive actually overdrives the local current density. Both NBCD over- and under-drive have both been demonstrated in AT plasmas differing in confinement. This suggests the possibility of developing some measure of bipolar transport control with the capability of either increasing or decreasing transport. With slight improvements to confinement to reduce the neutral beam power demand, and with additional duration, the inductive current profile is expected to fully relax to zero.

Several hardware improvements are planned to foster further advances in the science of Advanced Tokamaks. A double-null pumped divertor will allow operation with an optimized shape. Additional rf power is planned, with increases to 9 MW of EC and 5 MW of fast wave. This will allow demonstration of steady state regimes for as long as 10 seconds, or several current relaxation times. Replacing some of the NBI with rf will facilitate operation with  $T_{\text{e}} \approx T_{\text{i}}$ . Finally, two (out of eight) NBI sources are planned to be re-aimed in the counter direction. This will give added flexibility by allowing us to vary the co/counter mix of NBI sources, thereby modifying both NBCD and rotation. Scenarios approaching 100% bootstrap current may be possible when NBCD is removed by balanced injection.

## References

- [1] M.R. Wade, T.C. Luce, P.A. Politzer, J.R. Ferron, *et al.*, “Progress toward long-pulse high-performance Advanced Tokamak discharges on the DIII-D tokamak,” *Phys. Plasmas* **8**, 2208 (2001).
- [2] C.M. Greenfield, M. Murakami, J.R. Ferron, M.R. Wade, T.C. Luce, C.C. Petty, J.E. Menard, T.W. Petrie, S.L. Allen, K.H. Burrell, T.A. Casper, J.C. DeBoo, E.J. Doyle, A.M. Garofalo, I.A. Gorelov, R.J. Groebner, J. Hobirk, A.W. Hyatt, R.J. Jayakumar, C.E. Kessel, R.J. La Haye, G.L. Jackson, J. Lohr, M.A. Makowski, R.I. Pinsker, P.A. Politzer, R. Prater, E.J. Strait, T.S. Taylor, W.P. West, and the DIII-D Team, “High performance advanced tokamak regimes in DIII-D,” *Phys. Plasmas* **11**, 2616 (2004).
- [3] X. Litaudon, A. Bécoulet, F. Crisanti, R.C. Wolf, *et al.*, “Progress towards steady-state operation and real-time control of internal transport barriers in JET,” *Nucl. Fusion* **43**, 565 (2003).
- [4] S. Ishida, JT-60 Team and JFT-2M Group, “High-beta steady-state research and future directions on the Japan Atomic Energy Research Institute Tokamak-60 Upgrade and the Japan Atomic Energy Research Institute Fusion Torus-2 Modified,” *Phys. Plasmas* **11**, 2532 (2004).
- [5] T.C. Luce, M.R. Wade, J.R. Ferron, P.A. Politzer, A.W. Hyatt, A.C.C. Sips, and M. Murakami, “High performance stationary discharges in the DIII-D tokamak,” *Phys. Plasmas* **11**, 2627 (2004).
- [6] C. Gormezano, “Hybrid advanced scenarios: Perspectives for ITER and experiments with dominant RF heating,” submitted to *Plasma Physics and Control. Fusion* (2004).
- [7] R.J. Bickerton, J.W. Connor, J.B. Taylor, *Nature Phys. Sci.* **229**, 110 (1971).
- [8] A.D. Turnbull, M.S. Chu, T.S. Taylor, T.A. Casper, *et al.*, *Proceedings of the 16th Fusion Energy Conference*, Montreal, 1996, Vol. 2 (International Atomic Energy Agency, Vienna, 1997) p. 509.
- [9] M.A. Makowski, T.A. Casper, J.R. Ferron, T.S. Taylor, and A.D. Turnbull, “Effect of Profiles and Shape on Ideal Stability of Advanced Tokamak Equilibria,” in *Proceedings of the 30th European Conference on Controlled Fusion and Plasma Physics*, St. Petersburg, 2003, ECA Vol. 27A (European Physical Society, Geneva: EPS2003), P-2.113, [http://eps2003.ioffe.ru/PDFS/P2\\_113.PDF](http://eps2003.ioffe.ru/PDFS/P2_113.PDF).
- [10] C.E. Kessel, J.R. Ferron, C.M. Greenfield, J.E. Menard, and T.S. Taylor, “Shape Optimization for DIII-D Advanced Tokamak Plasmas,” in *Proceedings of the 30th European Conference on Controlled Fusion and Plasma Physics*,

- St. Petersburg, 2003, ECA Vol. 27A (European Physical Society, Geneva: EPS2003), P-4.044, [http://eps2003.ioffe.ru/PDFS/P4\\_044.PDF](http://eps2003.ioffe.ru/PDFS/P4_044.PDF).
- [11] A.M. Garofalo, T.H. Jensen, L.C. Johnson, R.J. La Haye, G.A. Navratil, M. Okabayashi, J.T. Scoville, E.J. Strait, D.R. Baker, J. Bialek, M.S. Chu, J.R. Ferron, R.J. Jayakumar, L.L. Lao, M.A. Makowski, H. Reimerdes, T.S. Taylor, A.D. Turnbull, M.R. Wade, and S.K. Wong, “*Sustained rotational stabilization of DIII-D plasmas above the no-wall beta limit*,” Phys. Plasmas **5**, 1997 (2002).
- [12] E.J. Strait, J. Bialek, I.N. Bogatu, M.S. Chance, et al., “*Resistive wall mode stabilization with internal feedback coils in DIII-D*,” Phys. Plasmas **11**, 2505 (2004).
- [13] A.M. Garofalo, et al., in *Proceedings of the 31<sup>st</sup> European Conference on Controlled Fusion and Plasma Physics*, London, 2004, (European Physical Society, Geneva: EPS2004).
- [14] R.J. La Haye, S. Günter, D.A. Humphreys, J. Lohr, et al., “*Control of neoclassical tearing modes in DIII-D*,” Phys. Plasmas **9**, 2051 (2002).
- [15] C.C. Petty, R.J. La Haye, T.C. Luce, D.A. Humphreys, et al., “*Complete suppression of the  $m=2/n=1$  neoclassical tearing mode using electron cyclotron current drive on DIII-D*,” Nucl. Fusion **44**, 243 (2004).
- [16] G. Gantenbein, H. Zohm, G. Giruzzi, S. Günter, et al., “*Complete Suppression of Neoclassical Tearing Modes with Current Drive at the Electron-Cyclotron-Resonance Frequency in ASDEX Upgrade Tokamak*,” Phys. Rev. Lett. **85**, 1242 (2000).
- [17] A. Isayama, Y. Kamada, S. Ide, K. Hamamatsu, et al., “*Complete stabilization of a tearing mode in steady state high- $\beta_p$  H-mode discharges by the first harmonic electron cyclotron heating/current drive on JT-60U*,” Plasma Phys. Controlled Fusion **42**, L37 (2000).
- [18] R.J. La Haye, et al., in *Proceedings of the 31<sup>st</sup> European Conference on Controlled Fusion and Plasma Physics*, London, 2004, (European Physical Society, Geneva: EPS2004).
- [19] M. Murakami, M.R. Wade, J.C. DeBoo, C.M. Greenfield, et al., “*Advanced tokamak profile evolution in DIII-D*,” Phys. Plasma **10**, 1691 (2003).
- [20] T.S. Taylor, “*Physics of advanced tokamaks*,” Plasma Phys. Control. Fusion **39**, B47 (1997).
- [21] M. Murakami, M.R. Wade, C.M. Greenfield, T.C. Luce, et al., “*Modification of the current profile in high-performance plasmas using off-axis electron-cyclotron-current drive in DIII-D*,” Phys. Rev. Lett. **90**, 255001 (2003).
- [22] E.A. Lazarus, L.L. Lao, T.H. Osborne, T.S. Taylor, et al., “*An optimization of beta in the DIII-D tokamak*,” Phys. Fluids B **4**, 3644 (1992).
- [23] J.R. Ferron, D.P. Brennan, T.A. Casper, A.M. Garofalo, et al., in *Proceedings of the 29th European Conference on Controlled Fusion and Plasma Physics*,

- Montreaux, 2002, (European Physical Society, Geneva: EPS2002), [http://elise.epfl.ch/pdf/P1\\_060.pdf](http://elise.epfl.ch/pdf/P1_060.pdf).
- [24] M.S. Chu, A. Bondeson, M.S. Chance, Y.Q. Liu, et al., “*Modeling of Feedback and Rotation Stabilization of the Resistive Wall Mode in Tokamaks*,” Phys. Plasmas **11**, 2497 (2004).
- [25] C.C. Petty, R. Prater, T.C. Luce, R.A. Ellis, et al., “*Effects of electron trapping and transport on electron cyclotron current drive on DIII-D*,” Nucl. Fusion **43**, 700 (2003).
- [26] B.W. Rice, K.H. Burrell, L.L. Lao, Y.R. Lin-Liu, et al., “*Direct measurement of the radial electric field in tokamak plasmas using the Stark effect*,” Phys. Rev. Lett. **79**, 2694 (1997).
- [27] E.J. Doyle, G.M. Staebler, L. Zeng, T.L. Rhodes, et al., “*Observation of simultaneous internal transport barriers in all four transport channels and correlation with turbulence behaviour in NCS discharges on DIII-D*,” Plasma Phys. Control. Fusion **42**, A237 (2000).
- [28] R.I. Pinsky, et al., in *Proceedings of the 31<sup>st</sup> European Conference on Controlled Fusion and Plasma Physics*, London, 2004, (European Physical Society, Geneva: EPS2004).
- [29] E.J. Doyle, C.M. Greenfield, M.E. Austin, L.R. Baylor, et al., “*Progress towards increased understanding and control of internal transport barriers in DIII-D*,” Nucl. Fusion **42**, 333 (2002).
- [30] X. Garbet, “*Physics of Transport in Tokamaks*,” submitted to Plasma Physics and Control. Fusion (2004).
- [31] T.S. Hahm and K.H. Burrell, “*Behaviour of electron and ion transport in discharges with an internal transport barrier in the DIII-D tokamak*,” Phys Plasmas **2**, 1648 (1995).
- [32] C.M. Greenfield, J.C. DeBoo, T.C. Luce, B.W. Stallard, E.J. Synakowski, et al., “*Understanding and control of transport in Advanced Tokamak regimes in DIII-D*,” Phys. Plasmas **7**, 1959 (2000).
- [33] R.E. Waltz, G.M. Staebler, W. Dorland, G.W. Hammett, et al., “*A gyro-Landau-fluid transport model*,” Phys. Plasmas **4**, 2482 (1997).
- [34] M.A. Beer, G.W. Hammett, G. Rewoldt, E.J. Synakowski, M.C. Zarnstorff, W. Dorland, “*Gyrofluid simulations of turbulence suppression in reversed-shear experiments on the Tokamak Fusion Test Reactor*,” Phys. Plasmas **4**, 1792 (1997).
- [35] C.M. Greenfield, K.H. Burrell, T.A. Casper, J.C. DeBoo, et al., “*Improvement of Core Barriers with ECH and Counter-NBI in DIII-D*,” in *Proceedings of the 27th European Conference on Controlled Fusion and Plasma Physics*, Budapest, 2000, Vol. 24B (European Physical Society, Budapest, 2000), p.544.

- [36] L.R. Baylor, T.C. Jernigan, S.K. Combs, W.A. Houlberg, M. Murakami, et al., “Improved core fueling with high field side pellet injection in the DIII-D tokamak,” *Phys. Plasmas* **7**, 1878 (2000).
- [37] C.M. Greenfield, C.L. Rettig, G.M. Staebler, B.W. Stallard, et al., “Behaviour of electron and ion transport in discharges with an internal transport barrier in the DIII-D tokamak,” *Nucl. Fusion* **39**, 1723 (1999).
- [38] M.R. Wade, M. Murakami, T. C. Luce, J.R. Ferron, et al., “Integrated, advanced tokamak operation on DIII-D,” *Nucl. Fusion* **43**, 634 (2003).
- [39] T.W. Petrie, J.G. Watkins, S.L. Allen, N.H. Brooks, et al., “Changes in particle pumping due to variation in magnetic balance near double-null in DIII-D,” in *Proceedings of the 30th European Conference on Controlled Fusion and Plasma Physics*, St. Petersburg, 2003, ECA Vol. 27A (European Physical Society, Geneva: EPS2003), P-4.086, [http://eps2003.ioffe.ru/PDFS/P4\\_086.PDF](http://eps2003.ioffe.ru/PDFS/P4_086.PDF).
- [40] D.A. Humphreys, J.R. Ferron, A.M. Garofalo, A.W. Hyatt, T.C. Jernigan, R. Johnson, R.J. La Haye, J.A. Leuer, M. Okabayashi, B.G. Penafior, J.T. Scoville, E.J. Strait, M.L. Walker, D.G. Whyte, “Advanced Tokamak Operation Using the DIII-D Plasma Control System,” *Proc. 22nd Symp. on Fusion Technol.*, Helsinki, Finland, September 2002; *Fus. Eng. Des.* **66-68**, 663 (2003).
- [41] M.R. Wade, M. Murakami, J.R. Ferron, J. Lohr, et al., *Bull. Am. Phys. Soc.* **47**, 226 (2002).
- [42] J.R. Ferron, M.L. Walker, L.L. Lao, H.E. St John, D.A. Humphreys, J.A. Leuer, “Real Time Equilibrium Reconstruction for Tokamak Discharge Control,” *Nucl. Fusion* **38**, 1055 (1998).
- [43] ITER Physics Expert Group on Confinement and Transport, ITER Physics Expert Group on Confinement Modeling and Database and ITER Physics Basis Editors, “Chapter 2: Plasma confinement and transport,” *Nucl. Fusion* **39**, 2175 (1999).
- [44] J.E. Kinsey, G.M. Staebler, R.E. Waltz, “Burning Plasma Confinement Projections and Renormalization of the GLF23 Drift-Wave Transport Model,” *Fusion Sci. Technol.* **44**, 763 (2003).
- [45] M. Murakami, J.C. DeBoo, J.R. Ferron, C.M. Greenfield, et al., *Bull. Am. Phys. Soc.* **48**, 129 (2003).
- [46] H.E. St. John, T.S. Taylor, Y.R. Lin-Liu, and A.D. Turnbull, *Plasma Physics and Controlled Nuclear Fusion Research 1994*, in *Proceedings of the 15th IAEA Conference*, Seville, 1994, Vol. 3 (IAEA, Vienna, 1994) p. 603.
- [47] R.J. Hawryluk, “An empirical approach to tokamak transport,” in *Physics Close to Thermonuclear Conditions*, edited by B. Coppi et al. (Commission of the European Communities, Brussels, 1980), Vol. 1, p. 19.
- [48] W.A. Houlberg, K.C. Shaing, S.P. Hirshman, M.C. Zarnstorff, “Bootstrap current and neoclassical transport in tokamaks of arbitrary collisionality and aspect ratio,” *Phys. Plasmas* **4**, 3230 (1997).

- [49] O. Sauter, C. Angioni, and Y.R. Lin-Liu, “*Neoclassical conductivity and bootstrap current formulas for general axisymmetric equilibria and arbitrary collisionality regime*,” Phys. Plasmas **6**, 2834 (1999).
- [50] K. Matsuda, “*Ray tracing study of the electron cyclotron current drive in DIII-D using 60 GHz*,” IEEE Trans. Plasma Sci. **17**, 6 (1989).
- [51] L.L. Lao, J.R. Ferron, J.R. Groebner, W.W. Howl, H.E. St. John, E.J. Strait, T.S. Taylor, Nucl. Fusion **30**, 1035 (1990).
- [52] C.B. Forest, K. Kupfer, T.C. Luce, P.A. Politzer, L.L. Lao, M.R. Wade, D.G. Whyte, and D. Wròblewski, “*Determination of the Noninductive Current Profile in Tokamak Plasmas*,” Phys. Rev. Lett. **73**, 2444 (1994).
- [53] E.J. Synakowski, S.H. Batha, M.A. Beer, M.G. Bell, et al., “*Roles of electric field shear and Shafranov shift in sustaining high confinement in enhanced reversed shear plasmas on the TFTR tokamak*,” Phys. Rev. Lett. **78**, 2972 (1997).
- [54] H. Shirai, M. Kikuchi, T. Takizuka, T. Fujita, et al., “*Role of radial electric field and plasma rotation in the time evolution of internal transport barrier in JT-60U*,” Plasma Phys. Control Fusion **42**, A109 (2000).

## **Acknowledgment**

This is a report of work supported by the U.S. Department of Energy under Contract Nos. DE-FC02-04ER54698, DE-AC05-00OR22725, DE-AC02-76CH03073, W-7405-ENG-48, DE-FG03-01ER54615, and DE-FG02-89ER53297. The authors would like to thank the DIII-D Operations Group, and in particular the ECH Group, for help in carrying out the described experiments.